Optimization of Active Layer Thickness in Planar Organic Solar Cells via Optical Simulation Methods

Optimization of Active Layer Thickness in Planar Organic Solar Cells via Optical Simulation Methods

Patrick Boland and Gon Namkoong*

Department of Electrical and Computer Engineering, Applied Research Center, Old Dominion University, Newport News, VA 23606, U.S.A.

Received November 7, 2009; accepted January 24, 2010; published online March 5, 2010

A thin-film optical simulation modeling has been used to determine ideal active layer thicknesses for regioregular poly(3-hexylthiophene) and phenyl-C_{61}/C_{71}-butyric acid methyl ester (P3HT:PC_{61}BM and P3HT:PC_{71}BM) organic blends used as photoactive components in polymer solar cells. Solar cells are simulated based on their optical properties after varying such factors as active layer thickness, electron and hole mobilities, and the Langevin recombination efficiency. Our results indicate that optimizing device efficiency is strongly dependent on the simultaneous control of active layer thickness and the charge carrier mobilities.

DOI: 10.1143/JJAP.49.030205

There are considerable data in the literature describing the significance of active layer thickness and its impact on the efficiency of bulk-heterojunction organic solar cells.[1–4] However, some incongruity exists regarding the optimal thickness required to achieve maximum energy conversion efficiency.[1–3] For example, Li *et al.* found that energy conversion efficiency and short circuit current density of regioregular poly(3-hexylthiophene) and phenyl-C_{61}-butyric acid methyl ester (P3HT:PC_{61}BM) peaked at a layer thickness of 63 nm.[1] However, other researchers have tested similarly constructed devices and found that in some cases efficiency actually showed near-constant efficiencies over a wide thickness range (50–400 nm).[2,4] In addition to the optimal thickness, current research shows promising results with P3HT:PC_{71}BM devices yielding higher absorption and increased power conversion efficiencies compared to P3HT:PC_{61}BM-based solar cells.[5] Indeed, P3HT:PC_{71}BM shows greater absorption across a broader range of the visible spectrum due to the asymmetric structure of C_{71} fullerene that improves optical properties.[6,7] Therefore, device efficiency of PC_{71}BM-based organics compared to PC_{61}BM-based ones is shown to increase while the comparison of device performance between P3HT:PC_{61}BM and P3HT:PC_{71}BM solar cells is not well investigated.

In this paper we describe modeling and simulation of organic photovoltaic (OPV) devices using a software tool (Setfos3) that implements the transfer matrix method (TMM) and organic semiconductor drift-diffusion modules in layered thin-film OPVs.[8] The layer sequence for the devices used in all simulations followed a standard configuration: indium tin oxide (ITO) (120 nm)/poly(3,4-ethylenedioxythiophene):poly(styrene sulfonate) (PEDOT:PSS) (50 nm)/P3HT:PCBM (variable)/aluminum (100 nm). Complex indices of refraction over the wavelength range from 350 to 1000 nm were used in the optical calculations. We used real and imaginary parts of the complex refractive indexes for the P3HT:PC_{61}BM and P3HT:PC_{71}BM blends obtained from ref. 9. Molecular orbital energy levels for the P3HT:PCBM layers were set to values reported in the literature.[10] In pristine organic semiconductors, bimolecular free charge carrier recombination occurs and is described by the rate equation $R = \eta np(\mu_n + \mu_p)q/\varepsilon$, where n and p are electron and hole densities, q is the elementary charge, and ε is the material dielectric constant.[11,12] In this simulation, the Langevin recombination parameter $\eta = 0.1$ is used to weight the rate equation in order to mimic realistic conditions found with polymer–fullerene blends.[11,13]

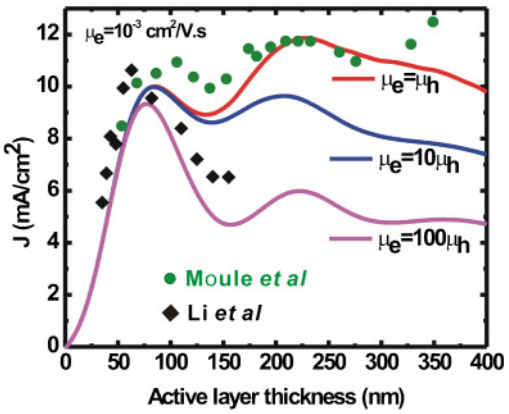

Fig. 1. (Color online) Current density as a function of active layer thickness for three combinations of electron/hole mobilities ($\mu_e = \mu_h = 10^{-3}$ cm^2 V^{-1} s^{-1}, $\mu_e = 10\mu_h$, $\mu_e = 100\mu_h$) in P3HT:PC_{61}BM and experimental data from Li[1] and Moule *et al.*[4]

Figure 1 shows simulated current densities for P3HT:PC_{61}BM as a function of layer thickness along with experimental data from Li[1] and Moule *et al.*[4] which showed energy conversion efficiencies over 4%. Three combinations of electron/hole mobilities are shown: 1) $\mu_e = \mu_h = 10^{-3}$ cm^2 V^{-1} s^{-1}, 2) $\mu_e = 10\mu_h$, and 3) $\mu_e = 100\mu_h$. At a range of about 80–100 nm, the current densities for each are relatively close in value. The oscillations in the current density can be attributed to variations in carrier generation rate inside the active layer where interference occurs by the opaque electrode.[1] However, distinctly different current densities have been observed that depend upon carrier mobilities and increased thickness. For the carrier mobility where $\mu_e = \mu_h = 10^{-3}$ cm^2 V^{-1} s^{-1}, the current densities keep increasing with increased device thickness while the decline of the current densities dominates when the hole mobilities drop by one or two orders of magnitude compared to that of the electron. Furthermore, the close correlation between simulated and experimental data from Li[1] and Moule *et al.*[4] indicates the validity of our simulation model.

As can be seen in Fig. 2, manipulation of the active layer thickness has a marked impact on short circuit current density (J_{SC}) and, to a lesser extent, on open circuit voltage (V_{OC}) and subsequently either increases or decreases the fill factor (FF)

*E-mail address: gnamkoon@odu.edu

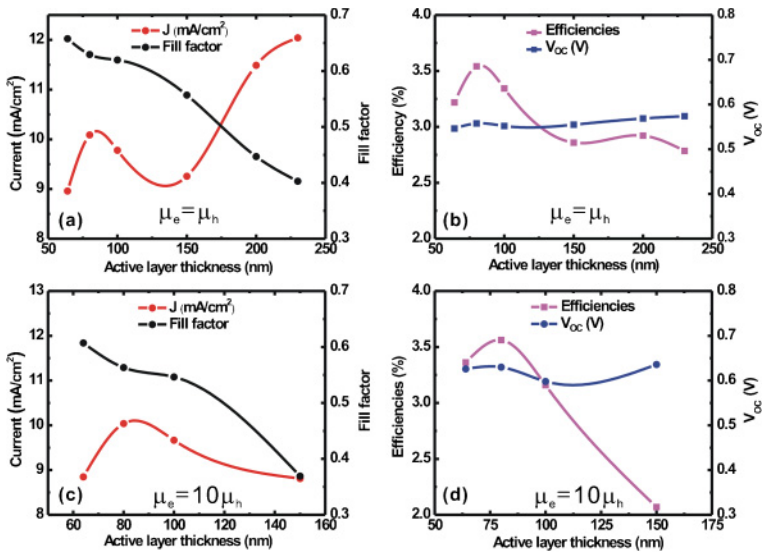

Fig. 2. (Color online) Electrical characteristics for P3HT:$PC_{61}BM$ simulations: (a) J_{SC} and FF vs active layer thickness, (b) efficiency and V_{OC} vs active layer thickness for $\mu_e = \mu_h = 10^{-3}\,cm^2\,V^{-1}\,s^{-1}$, (c) J_{SC} and FF vs active layer thickness, and (d) efficiency and V_{OC} vs active layer thickness for $\mu_e = 10\mu_h = 10^{-3}\,cm^2\,V^{-1}\,s^{-1}$.

and efficiency. When carrier mobilities in P3HT:$PC_{61}BM$ simulations are equal to $\mu_e = \mu_h = 10^{-3}\,cm^2\,V^{-1}\,s^{-1}$, V_{OC} remains virtually constant while the fill factor trends almost linearly downward from a maximum of 0.65 in Figs. 2(a) and 2(b). This decline in FF is attributable to the increase in device resistance that results from increased layer thickness. Current density declines from the maximum over a short thickness range but then once again increases significantly. This increase in current density and corresponding decline in fill factor causes the efficiency to remain essentially constant across the expanse of the active layer. Therefore, it is found that a maximum efficiency of ~3.5% was observed with 80–100 nm active layer thickness. When the magnitude of the hole mobility is decreased by a factor of 10 ($\mu_e = 10\mu_h = 10^{-3}\,cm^2\,V^{-1}\,s^{-1}$), effects on FF, efficiency, and current density are pronounced as shown in Figs. 2(c) and 2(d). The maxima seen with equal mobility combinations remain, but the subsequent declines with increasing thickness are much faster and no secondary increase in current density is observed. Because both FF and current density decrease simultaneously, efficiency no longer remains constant but rather falls off more rapidly.

Figures 3(a) and 3(b) show values for efficiency as a function of active layer thickness for two sets of electron/hole mobility combinations in P3HT:$PC_{61}BM$. It is clear a strong dependence between carrier mobilities, thickness, and efficiency exists. The highest efficiencies are found when carrier mobility for both electrons and holes is the same — even if the *magnitude* of the mobilities is different. As the electron/hole mobility ratios change and become greater, there is a corresponding decrease in both efficiency and optimal layer thickness. The effects are most apparent when there is at least a two orders of magnitude difference between the electron and hole mobilities. The optimal active layer thickness shifts from ~80 nm with $\mu_e = \mu_h$ to ~60 nm when $\mu_e = 100\ \mu_h = 10^{-3}\,cm^2\,V^{-1}\,s^{-1}$. In Fig. 3(b), when electron mobility is dropped to $10^{-4}\,cm^2\,V^{-1}\,s^{-1}$, overall efficiency declines below 3% in each case from that observed with $\mu_e = 10^{-3}$ where the maximum efficiencies were ~3.5%. In both figures,

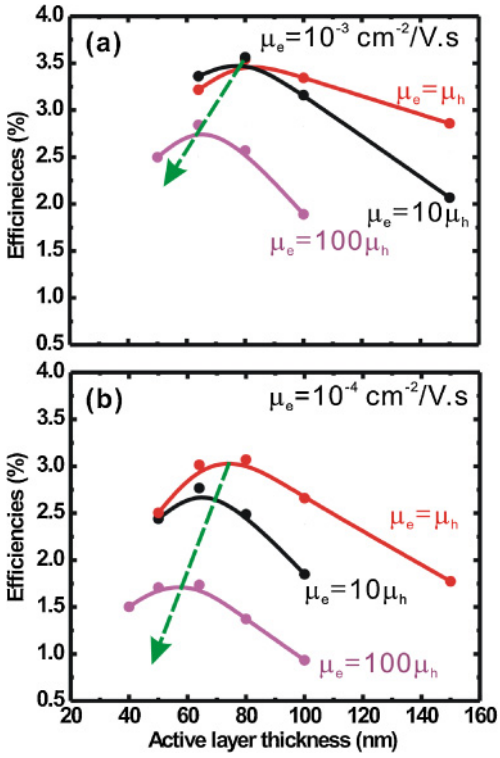

Fig. 3. (Color online) P3HT:$PC_{61}BM$ device efficiencies as a function of active layer thickness for (a) $\mu_e = \mu_h = 10^{-3}\,cm^2\,V^{-1}\,s^{-1}$, $\mu_e = 10\mu_h$, $\mu_e = 100\mu_h$, and (b) $\mu_e = \mu_h = 10^{-4}\,cm^2\,V^{-1}\,s^{-1}$, $\mu_e = 10\mu_h$, $\mu_e = 100\mu_h$.

the largest decline in efficiency occurs with a two-order-of-magnitude difference in carrier mobilities. This is primarily due to carrier recombination and, at these lower mobilities, to space charge limited current affects (SCLC).[3] SCLC becomes prominent when hole mobility differs from that of the electrons by two orders of magnitude or more[12] leading to unbalanced distribution of charge carriers across the active layer. Therefore, the effects of SCLC significantly influence fill factor and the decline in current density, thereby resulting in a drastic reduction of efficiency.

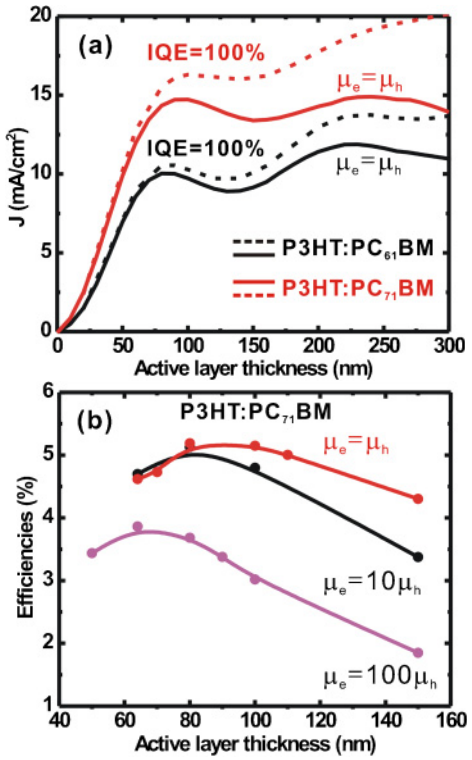

Fig. 4. (Color online) (a) Comparison of J_{SC} vs active layer thickness for internal quantum efficiency (IQE) = 100 (dotted lines) and P3HT:PC_{61}BM and P3HT:PC_{71}BM mobilities (solid lines) equal to $\mu_e = \mu_h = 10^{-3}\,cm^2\,V^{-1}\,s^{-1}$. (b) P3HT:$PC_{71}$BM efficiency vs active layer thickness for $\mu_e = \mu_h = 10^{-3}\,cm^2\,V^{-1}\,s^{-1}$, $\mu_e = 10\mu_h$, and $\mu_e = 100\mu_h$.

Our simulation model did not include the various morphologies of organic blends that are known to affect electrical and optical properties. Optimal morphologies of P3HT:PCBM organic blends are found with a blend ratio of approximately 1 : 1 leading to fine intermixing between donor and acceptor constituents.[15] It is found that morphologies using other blend ratios lead to large scale sub-domains resulting in inefficient exciton dissociation and diminished charge collection and absorption efficiencies. For example, 1 : 2 compositions of P3HT:PCBM result in a coarser mixture while 1 : 4 compositions developed PCBM-rich, sub-micron scale domains.[15] Even though PCBM-rich domains resulting from higher PCBM concentrations improved charge collection efficiencies due to relatively higher electron mobility of PCBM, diminished light absorption efficiencies and reduced interfacial surface area between P3HT:PCBM decreased the overall energy conversion efficiencies as compared to organic blends with morphologies developed with a blend ratio of 1 : 1.[15] In the case of P3HT-rich morphologies, poor exciton dissociation degrades energy conversion efficiencies.[15] As a result, increased active layer thickness in organic blends that deviate significantly from a ratio of 1 : 1 will lead to reduced optimal layer thickness.

Figure 4 shows simulated data for P3HT:PC_{71}BM contrasted with P3HT:PC_{61}BM. Graphs of current density and efficiency as functions of active layer thickness and open circuit voltage show the potential for PC_{71}BM to eclipse PC_{61}BM due to its superior optical and electrical properties. Figure 4(a) shows the two different blends having equal charge carrier mobilities in each (i.e., $\mu_e = \mu_h = 10^{-3}$ $cm^2\,V^{-1}\,s^{-1}$). Current densities when internal quantum efficiency (IQE) is 100% are shown for both with that for PC_{71}BM being approximately 55% greater in the 80–100 nm thickness range. For a real device produced in our lab, the current density of P3HT:PC_{71}BM was 35% greater than that for PC_{61}BM.[16] Simulated efficiencies as a function of active layer thickness are much improved in P3HT:PC_{71}BM yielding more than 5% compared to 3.5% for P3HT:PC_{61}BM [Fig. 4(b)]. With a one order of magnitude ($\mu_e = 10\mu_h$) change in carrier mobility, efficiencies remain high with a slight downward shift in optimal thickness to about 80 nm. Even with an increase in thickness to 150 nm, efficiency only drops to 3.5% — still close to the efficiency of P3HT:PC_{61}BM at its optimal active layer thickness for the same carrier mobilities [Fig. 3(a)]. Again, a two-order-of-magnitude difference in electron/hole mobility ratio produces a more significant decline in efficiency and reduction in optimal layer thickness due to recombination and SCLC.

In summary, optical simulation and modeling of polymer active layers in organic solar cells has been performed to determine the most effective thicknesses and charge carrier mobilities enabling maximum efficiency to be achieved. Complex refractive index data and realistic electron and hole mobilities were systematically varied to simulate the function of P3HT:PC_{61}BM and P3HT:PC_{71}BM organic blend layers used as photoactive components in polymer solar cells. Spectral absorption, fill factor, efficiency, and current–voltage characteristics were obtained for both donor/acceptor blends and optimal thicknesses determined to attain maximum efficiency. P3HT:PC_{71}BM shows the greatest potential for higher efficiencies at thicknesses around 100 nm compared to P3HT:PC_{61}BM that shows highest efficiency at approximately 80 nm. It is found that optimum layer thickness is strongly dependent upon the magnitude and ratio of charge carrier mobilities.

1) G. Li, V. Shrotriya, Y. Yao, and Y. Yang: J. Appl. Phys. **98** (2005) 043704.
2) A. J. Moule, J. B. Bonekamp, and K. Meerholz: J. Appl. Phys. **100** (2006) 094503.
3) M. Lenes, L. J. A. Koster, V. D. Mihailetchi, and P. W. M. Blom: Appl. Phys. Lett. **88** (2006) 243502.
4) A. J. Moule and K. Meerholz: Appl. Phys. B **92** (2008) 209.
5) T. Yamanari, T. Taima, J. Sakai, and K. Saito: Jpn. J. Appl. Phys. **47** (2008) 1230.
6) J. Peet, J. Y. Kim, N. E. Coates, W. L. Ma, D. Moses, A. J. Heeger, and G. C. Bazan: Nat. Mater. **6** (2007) 497.
7) M. M. Wienk, J. M. Kroon, W. J. H. Verhees, J. Knol, J. C. Hummelen, P. A. van Hall, and R. A. J. Janssen: Angew. Chem., Int. Ed. **42** (2003) 3371.
8) Semiconducting Thin Film Optics Simulation Software (Fluxim AG, 2006).
9) G. Dennler, K. Forberich, T. Ameri, C. Waldauf, P. Denk, C. J. Brabec, K. Hingerl, and A. J. Heeger: J. Appl. Phys. **102** (2007) 123109.
10) G. Dennler, M. C. Scharber, and C. J. Brabec: Adv. Mater. **21** (2009) 1323.
11) C. Deibel, A. Baumann, and V. Dyakonov: Appl. Phys. Lett. **93** (2008) 163303.
12) L. J. A. Koster, V. D. Mihailetchi, and P. W. M. Blom: Appl. Phys. Lett. **88** (2006) 052104.
13) C. Deibel, A. Baumann, A. Wagenpfahl, and V. Dyakonov: Synth. Met. **159** (2009) 2345.
14) C. Deibel, A. Wagenpfahl, and V. Dyakonov: Phys. Status Solidi: Rapid Res. Lett. **2** (2008) 175.
15) Y. Kim, S. A. Choulis, J. Nelson, D. D. C. Bradley, S. Cook, and J. R. Durrant: J. Mater. Sci. **40** (2005) 1371.
16) P. Boland, S. S. Sunkavalli, S. Chennuri, K. Foe, T. Abdel-Fattah, and G. Namkoong: Thin Solid Films **518** (2010) 1728.